

# Determination of $\overline{M_S}$ from quenched and $N_f = 2$ dynamical QCD

S. Booth<sup>a</sup>, M. Gockeler<sup>b</sup>, R. Horsley<sup>c</sup>, A. C. Irving<sup>d</sup>, B. Joo<sup>e 1</sup>,  
S. Pickles<sup>e 2</sup>, D. Pleiter<sup>c</sup>, P. E. L. Rakow<sup>b</sup>, G. Schierholz<sup>c,f</sup>,  
Z. Sroczynski<sup>e 3</sup>, H. Stuben<sup>g</sup>

{ QCD SF { UK QCD Collaboration {

<sup>a</sup>Edinburgh Parallel Computing Center EPCC,  
University of Edinburgh, Edinburgh EH9 3JZ, UK

<sup>b</sup>Institut für Theoretische Physik, Universität Regensburg,  
D-93040 Regensburg, Germany

<sup>c</sup>John von Neumann-Institut für Computing NIC,  
Deutsches Elektronen-Synchrotron DESY, D-15735 Zeuthen, Germany

<sup>d</sup>Theoretical Physics Division, Department of Mathematical Sciences,  
University of Liverpool, Liverpool L69 3BX, UK

<sup>e</sup>Department of Physics and Astronomy,  
University of Edinburgh, Edinburgh EH9 3JZ, UK

<sup>f</sup>Deutsches Elektronen-Synchrotron DESY, D-22603 Hamburg, Germany

<sup>g</sup>Konrad-Zuse-Zentrum für Informationstechnik Berlin, D-14195 Berlin, Germany

---

## Abstract

The scale parameter  $\overline{M_S}$  is computed on the lattice in the quenched approximation and for  $N_f = 2$  flavors of light dynamical quarks. The dynamical calculation is done with non-perturbatively  $O(a)$  improved Wilson fermions. In the continuum limit we obtain  $\frac{N_f=0}{\overline{M_S}} = 243(1)(10)$  MeV and  $\frac{N_f=2}{\overline{M_S}} = 217(16)(11)$  MeV, respectively.

Key words: QCD, Lattice, Strong coupling constant, parameter

PACS: 11.15.Ha, 12.38.-t, 12.38.Bx, 12.38.Gc

---

<sup>1</sup> Present address: Department of Physics, Columbia University, New York, NY 10027, USA

<sup>2</sup> Present address: Computer Services for Academic Research CSAR, University of Manchester, Manchester M13 9PL, UK

<sup>3</sup> Present address: Fachbereich Physik, Universität Wuppertal, D-42097 Wuppertal, Germany

## 1 Introduction

The parameter  $\Lambda_{\overline{MS}}$  sets the scale in QCD. In the chiral limit it is the only parameter of the theory, and hence it is a quantity of fundamental interest. Experimental information on  $\Lambda_{\overline{MS}}$  is obtained from the running of the strong coupling constant  $\alpha_s$  [1]. A theoretical determination requires non-perturbative techniques. In this letter we shall compute  $\Lambda_{\overline{MS}}$  on the lattice in the quenched approximation as well as for  $N_f = 2$  species of degenerate dynamical quarks.

Previous lattice calculations have employed a variety of methods to compute the strong coupling constant, in quenched and unquenched simulations. For reviews see [2,3]. The scale parameter  $\Lambda_{\overline{MS}}$  has been extracted from the heavy-quark potential [4,6], the quark-gluon vertex [7], the three-gluon vertex [8,9], from the spectrum of heavy quarkonia [10,14], and by means of finite-size-scaling methods [15].

We determine  $\Lambda_{\overline{MS}}$  from the average plaquette and the force parameter  $r_0$  [16]. Both quantities are widely computed in lattice simulations. In the quenched case we have many data points over a wide range of couplings at our disposal already, and in the dynamical case we expect to accumulate more points in the near future. At present  $r_0$  is the best known lattice quantity, at least in full QCD. It can easily be replaced with more physical scale parameters like hadron masses or  $f$  when the respective data become more accurate.

## 2 Method

The calculations are done with the standard gauge field action

$$S_G = \sum_x \text{Re} \frac{1}{3} \text{Tr} U_2(x); \quad (1)$$

and, in the dynamical case, with non-perturbatively  $O(a)$  improved Wilson fermions [17]

$$S_F = S_F^{(0)} - \frac{i}{2} \sum_x \text{Tr} c_{SW} a^4 \overline{\psi}(x) \not{D} \psi(x); \quad (2)$$

where  $S_F^{(0)}$  is the original Wilson action and  $\not{D} = \not{D} - g^2$ . If the improvement coefficient  $c_{SW}$  is appropriately chosen, this action removes all  $O(a)$  errors from on-shell quantities. A non-perturbative evaluation of this function leads to the parametrization [18]

$$c_{SW} = \frac{1 - 0.454g^2 - 0.175g^4 - 0.012g^6 + 0.045g^8}{1 - 0.720g^2} \quad (3)$$

for  $N_f = 2$  flavors, which is valid for  $g \leq 5.2$ .

The running of the coupling is described by the  $\beta$  function defined by

$$\frac{dg_S(\mu)}{d\ln\mu} = \beta^S(g_S(\mu)); \quad (4)$$

where  $S$  is any mass independent renormalization scheme. The perturbative expansion of the  $\beta$  function reads

$$\beta^S(g_S) = -\beta_0^S g_S^3 + \beta_1^S g_S^2 + \beta_2^S g_S^4 + \beta_3^S g_S^6 + \dots; \quad (5)$$

The first two coefficients are universal,

$$\begin{aligned} \beta_0^S &= \frac{1}{(4\pi)^2} [11 - \frac{2}{3}N_f]; \\ \beta_1^S &= \frac{1}{(4\pi)^4} [102 - \frac{38}{3}N_f]; \end{aligned} \quad (6)$$

while the others are scheme dependent. The renormalization group equation (4) can be exactly solved:

$$\frac{1}{g_S} = \beta_0^S g_S^2 \frac{b_1}{2b_0^2} \exp\left[\frac{1}{2\beta_0^S g_S^2} + \int_0^Z g_S d\ln\mu\right] \left[\frac{1}{\beta^S(\mu)} + \frac{1}{\beta_0^S} + \frac{b_1}{\beta_0^2}\right]; \quad (7)$$

where the scale parameter  $\mu$  appears as the integration constant. In the  $\overline{MS}$  scheme the  $\beta$  function is known to four loops [19]:

$$\begin{aligned} \beta_2^{\overline{MS}} &= \frac{1}{(4\pi)^6} \left[ \frac{2857}{2} N_f - \frac{5033}{18} + N_f^2 \frac{325}{54} \right]; \\ \beta_3^{\overline{MS}} &= \frac{1}{(4\pi)^8} \left[ \frac{149753}{6} + 3564 \zeta_3 - N_f \left( \frac{1078361}{162} + \frac{6508}{27} \zeta_3 \right) \right. \\ &\quad \left. + N_f^2 \left( \frac{50065}{162} + \frac{6472}{81} \zeta_3 \right) + N_f^3 \frac{1093}{729} \right]; \end{aligned} \quad (8)$$

where  $\zeta_3 = 1.20206$  is Riemann's zeta function.

In this paper we are concerned with three different schemes. In the continuum we use the  $\overline{MS}$  scheme. On the lattice we consider the bare coupling  $g(a)$  and the boosted coupling  $g_2(a)$ . The latter is given by

$$g_2^2(a) = \frac{g^2(a)}{P}; \quad (9)$$

where  $P = (1+3) \langle U_2 \rangle / \langle U_4 \rangle^2$  is the average plaquette value. The widespread opinion is that the perturbative expansion in  $g_2$  converges more rapidly than the expansion in the bare coupling [20]. Indeed, a comparison between the expansion coefficients in the two cases for the quenched plaquette shown in Fig. 1 supports this belief, as even for low orders the new series has oscillating

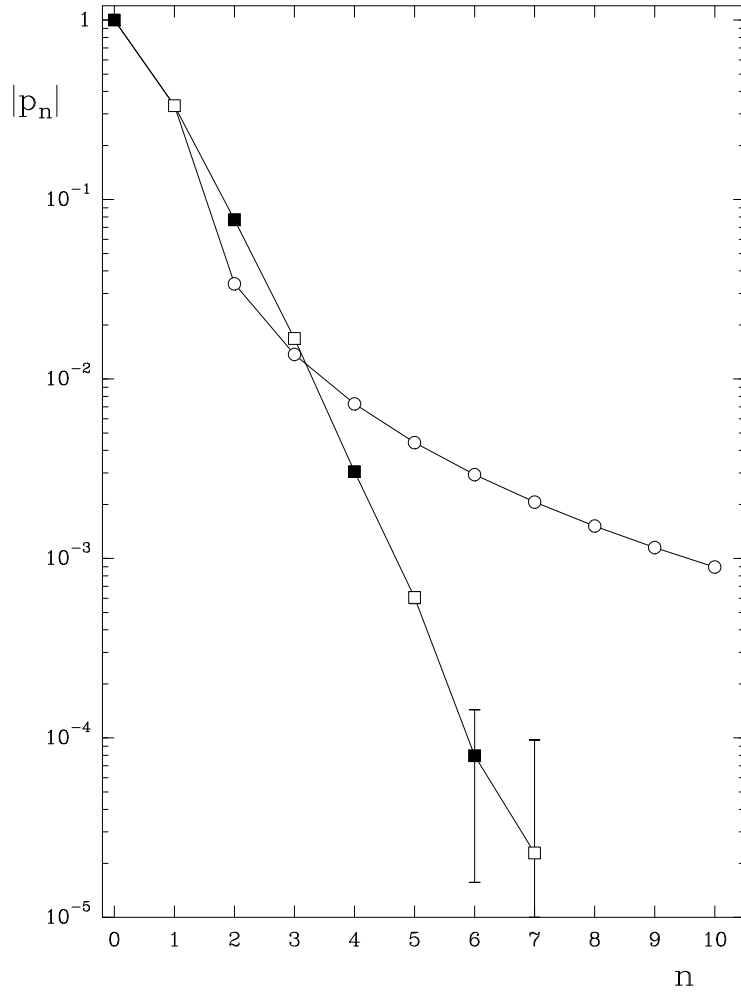


Fig. 1. The expansion coefficients for the quenched plaquette,  $1 - P = \sum_{n=1}^{\infty} P_n x^n$ , for  $x = g^2(a)$  (open circles) and  $x = g_2^2(a)$  (open squares), respectively. Open (solid) symbols refer to positive (negative) numbers. The bare expansion coefficients (open squares) are taken from [21]. Note that the boosted coefficients are not only much smaller and rapidly decreasing, but also alternating in sign.

coefficients. The conversion from the bare coupling to the  $\overline{MS}$  scheme has the form

$$\frac{1}{g_{\overline{MS}}^2(a)} = \frac{1}{g^2(a)} + 2b_0 \ln a + (b_1 + 2b_0 \ln a) g^2(a) + O(g^4 \ln^2 a): \quad (10)$$

Writing

$$\frac{1}{g_2^2} = \frac{1}{g^2} + b_1 g^2 + b_2 g^4 + \dots; \quad (11)$$

we obtain the relation between the boosted coupling and the  $\overline{MS}$  coupling

$$\frac{1}{g_{\overline{MS}}^2(\mu)} = \frac{1}{g_2^2(a)} + 2b_0 \ln a \left( \frac{\mu}{a} + p_1 \right) + (2b_1 \ln a \left( \frac{\mu}{a} + p_2 \right) + O(g^4 \ln^2 a)) : \quad (12)$$

By differentiating eq. (12) we can find the function coefficient,  $b_2^2$ , for the boosted coupling

$$b_2^2 = b_2^{\overline{MS}} + b_0 (p_2 - \frac{\mu}{a}) - b_1 (p_1 - \frac{\mu}{a}) : \quad (13)$$

The one-loop coefficients  $p_1$  and  $t_1$  are given by

$$p_1 = \frac{1}{3} ; \quad (14)$$

$$t_1 = 0.4682013 - N_f (0.0066960 - 0.0050467 g_W + 0.0298435 c_{SW}^2) + \text{am} (0.0272837 + 0.0223503 g_W - 0.0070667 c_{SW}^2) ; \quad (15)$$

where  $m$  is the quark mass. The quenched coefficients are taken from [22], whereas the fermionic contribution, including the improvement term proportional to  $\text{am}$ , is computed in the Appendix. The pure Wilson ( $c_{SW} = 0$ ) result agrees with [23], and the  $m = 0$  result agrees with the number quoted in [24]. The  $m = 0$  two-loop coefficients  $p_2$  and  $t_2$  are given by

$$p_2 = 0.033911 - \frac{8}{3} N_f (0.0006929 - 0.0000202 g_W + 0.0005962 c_{SW}^2) ; \quad (16)$$

$$t_2 = 0.0556675 + N_f (0.002600 - 0.000155 g_W + 0.012834 c_{SW}^2 + 0.000474 c_{SW}^3 + 0.000104 c_{SW}^4) : \quad (17)$$

The two-loop  $\text{am}$  term is not known. The quenched coefficients can be found in [22], whereas the fermionic contribution to  $p_2$  is given in [25], and  $t_2$  has been computed in [26].

Combining these terms gives

$$\frac{1}{g_{\overline{MS}}^2(\mu)} = \frac{1}{g_2^2(a)} + 2b_0 \ln a \left( \frac{\mu}{a} + (2b_1 \ln a \left( \frac{\mu}{a} + t_2 \right) + t_1) g_2^2(a) + \right. \quad (18)$$

with

$$t_1^2 = 0.1348680 - N_f (0.0066960 - 0.0050467 g_W + 0.0298435 c_{SW}^2) + \text{am} (0.0272837 + 0.0223503 g_W - 0.0070667 c_{SW}^2) ; \quad (19)$$

$$t_2^2 = 0.0217565 + N_f (0.000753 - 0.000209 g_W + 0.0144236 c_{SW}^2 + 0.000474 c_{SW}^3 + 0.000104 c_{SW}^4) : \quad (20)$$

Note that  $t_1^2 = t_1$ , so that the series converting  $g_2$  to  $g_{\overline{M S}}$ , eq. (18), is better behaved than the original series converting bare  $g$  to  $g_{\overline{M S}}$ , eq. (10). We can improve the convergence of the series further by re-expressing it in terms of the tadpole improved coefficients [20]

$$\begin{aligned} e_{SW} &= g_W u_0^3; \\ \overline{a\overline{m}} &= \overline{a\overline{m}}_0: \end{aligned} \quad (21)$$

We then obtain

$$\frac{1}{g_{\overline{M S}}^2(\overline{a})} = \frac{1}{g_2^2(a)} + 2b_0 \ln a \left( \overline{e}_1^2 + (2b_1 \ln a - \overline{e}_2^2) g_2^2(a) + \right. \quad (22)$$

with

$$\begin{aligned} \overline{e}_1^2 &= 0.1348680 - N_f (0.0066960 - 0.0050467 e_{SW} + 0.0298435 e_{SW}^2 \\ &+ \overline{a\overline{m}} (0.0272837 + 0.0223503 e_{SW} - 0.0070667 e_{SW}^2)); \end{aligned} \quad (23)$$

$$\begin{aligned} \overline{e}_2^2 &= 0.0217565 + N_f (0.000753 + 0.001053 e_{SW} - 0.000498 e_{SW}^2 \\ &+ 0.000474 e_{SW}^3 + 0.000104 e_{SW}^4); \end{aligned} \quad (24)$$

Changing  $t_1^2$  to  $\overline{e}_1^2$  is simply a matter of replacing every  $c_{SW}$  by  $e_{SW}$  and every  $\overline{m}$  by  $\overline{a\overline{m}}$ , but the change in  $t_2^2$  is not so simple, because the coefficients of the  $c_{SW}$  and  $c_{SW}^2$  terms change. We see that tadpole improvement is successful in reducing the two-loop fermionic contribution: the largest coefficient in the fermionic part of  $t_2^2$  was 0.01442 :::, in  $\overline{e}_2^2$  it is 0.00105 :::.

We are still free to choose the scale  $\overline{a}$  in eq. (22). A good value to help eq. (22) to converge rapidly is to choose  $\overline{a}$  so that the  $O(g^0)$  term vanishes. Therefore we choose the scale so that

$$\overline{a} = \exp \frac{\overline{e}_1^2}{2b_0}: \quad (25)$$

In the quenched case this gives  $\overline{a} = 2.63 = a$ , while for  $N_f = 2$  dynamical fermions  $\overline{a} = 1.4 = a$ . Substituting this scale into eq. (22), we obtain the relationship

$$g_{\overline{M S}}^2(\overline{a}) = g_2^2(a) + \overline{e}_2^2 \frac{b_1}{b_0} \overline{e}_1^2 g_2^6(a) + O(g^8); \quad (26)$$

which agrees with [22] in the quenched case.

The calculation of  $g_{\overline{M S}}$  proceeds in four steps. First we compute the average plaquette. From eq. (9) we then obtain  $g_2$ . In the second step we use eq. (26) to calculate  $g_{\overline{M S}}$  at the scale  $\overline{a}$ . Putting this value of  $g_{\overline{M S}}$  into eq. (7) gives us  $\overline{a} = \frac{1}{g_{\overline{M S}}}$ . Finally we use the conversion factor eq. (25) to turn this into a value for  $a_{\overline{M S}}$ . To convert our results to a physical scale, we use the force parameter  $r_0$ .

### 3 Results

$N_f = 0$

Let us begin with the quenched case. The plaquette values at  $\beta = 6.0, 6.2$  and  $6.4$  are taken from QCD SF's quenched simulations [27,28]. The  $r_0$  values are taken from [6,29]. At  $\beta = 5.95, 6.07$  and  $6.57$  the plaquette values are obtained by interpolation (in the former case using data at  $\beta = 5.85$  and  $5.8$  as well). In Fig. 2 we plot  $\frac{N_f=0}{M_S} r_0$  against  $(a=r_0)^2$ . The corresponding numbers are given in Table 1. The error is dominated by that in  $r_0$ , so the use of interpolated plaquette data is justified. One expects discretization errors of  $O(a^2)$ . Indeed, the data points lie on a straight line, allowing a linear extrapolation to the continuum limit. This gives

$$\frac{N_f=0}{M_S} r_0 = 0.616(2) \quad (27);$$

where the first error is purely statistical, while the second one is an estimate of the systematic error. The latter is derived by assuming that the higher-order contributions in eq. (26) are about 20% of the  $O(g^6)$  term. Using  $r_0 = 0.5 \text{ fm}$ ,

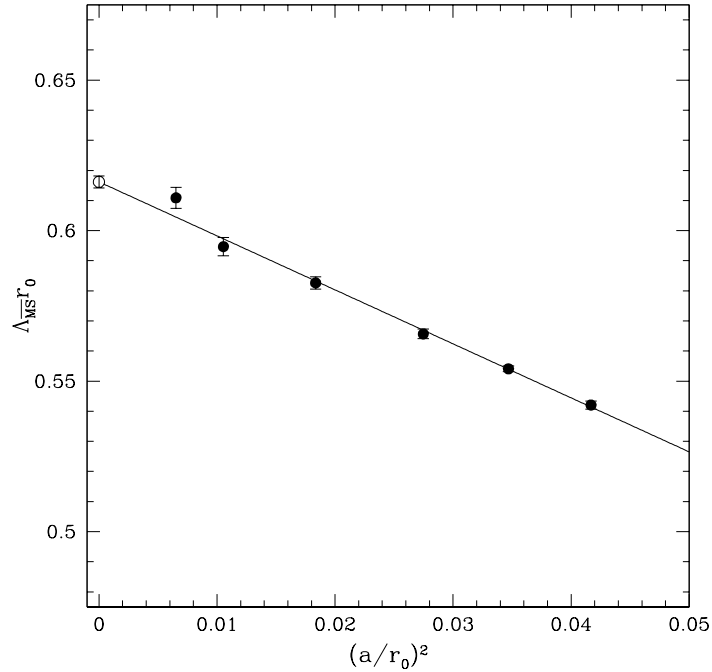


Fig. 2. The quenched scale parameter  $\frac{N_f=0}{M_S} r_0$  against  $(a=r_0)^2$  together with the continuum value (27). The coupling ranges from  $\beta = 5.95$  to  $6.57$ . The line is a linear extrapolation to the continuum limit.

	$\overline{M_S} r_0$	$(a=r_0)^2$
5.95	0.5421 (13)	0.04168 (20)
6.0	0.5541 (9)	0.03469 (12)
6.07	0.5657 (16)	0.02748 (16)
6.2	0.5826 (21)	0.01836 (13)
6.4	0.5947 (31)	0.01054 (11)
6.57	0.6109 (35)	0.00653 (7)

Table 1  
The quenched  $\overline{M_S} r_0$  values.

we find

$$\frac{N_f=0}{\overline{M_S}} = 243 (1) (10) \text{ M eV} \quad (28)$$

(which does not include any overall scale error). Our result agrees very well with the outcome of previous calculations [9,15]. Taking the mass to set the scale gives [28]  $r_0 = 0.52 (2) \text{ fm}$ , which is consistent with the value that is used here.

### $N_f = 2$

In the dynamical case we use combined results from the QCD SF and UKQCD collaborations [30,31]. The gauge field configurations were obtained using the standard Hybrid Monte Carlo algorithm with the non-perturbatively  $O(a)$  improved action (2). Details of the extraction of  $r_0=a$  will be given in [32]. For the quark mass we take the Ward identity mass. We compute this mass in the same way [33] as in the quenched case [27], with the improvement coefficient  $c_A$  taken from tadpole improved perturbation theory. The relevant parameters and results are given in Table 2.

As we are working at finite quark mass, we have to perform an extrapolation to the chiral limit. In Fig. 3 we show the parameter values of our simulations together with lines of constant  $r_0=a$  and  $m = m_c$ . This gives an impression of how far our simulations are from the chiral and continuum limits.

The value that interests us is  $\overline{M_S}$  at  $m \rightarrow 0$  and  $a \rightarrow 0$ . Given the fact that our action has discretization errors of  $O(a^2)$  only, at least as  $m \rightarrow 0$ , we expect the following small- $a$  behavior:  $\overline{M_S}(a) = \overline{M_S}(a=0) (1 + b_1 a m + O((a=r_0)^2) + O((am)^2))$ , where  $\overline{M_S}(a=0)$  is not supposed to depend on  $m$  anymore. Similarly, we expect to find  $r_0(a) = r_0(a=0) (1 + b_2 a m + O((a=r_0)^2) + O((am)^2))$ , with the difference that  $r_0(a=0)$  may still depend on  $m$ :  $r_0(a=0) = r_0(a=0; m=0) (1 + c_1 m r_0 + O((m r_0)^2))$ . Putting everything together,

	sea	V	c <sub>sw</sub>	P	r <sub>0</sub> =a	am	$\overline{M_S} r_0$
5.20	0.1355	16 <sup>3</sup> 32	2.0171	0.536294 (9)	5.041 (40)	0.02364 (16)	0.4744 (38)
5.20	0.1350	16 <sup>3</sup> 32	q	0.533676 (9)	4.754 (40)	0.04586 (19)	0.4593 (39)
5.25	0.1352	16 <sup>3</sup> 32	1.9603	0.541135 (24)	5.137 (49)	0.04268 (17)	0.4666 (45)
5.26	0.1345	16 <sup>3</sup> 32	1.9497	0.539732 (9)	4.708 (52)	0.07196 (20)	0.4348 (48)
5.29	0.1355	24 <sup>3</sup> 48	1.9192	0.547081 (26)	5.62 (9)	0.03495 (12)	0.4834 (77)
5.29	0.1350	16 <sup>3</sup> 32	q	0.545520 (29)	5.26 (7)	0.05348 (19)	0.4601 (61)
5.29	0.1340	16 <sup>3</sup> 32	q	0.542410 (9)	4.813 (45)	0.09272 (29)	0.4355 (41)

Table 2

The plaquette and  $r_0=a$  values together with the quark masses and our results for  $\overline{M_S} r_0$ . The improvement coefficient  $c_{sw}$  was taken from eq. (3).

we then arrive at the following parameterization of  $\overline{M_S} r_0$  for small  $a; m$  :

$$\overline{M_S} r_0 = A (1 + B am) (1 + C m r_0) + D (a=r_0)^2; \quad (29)$$

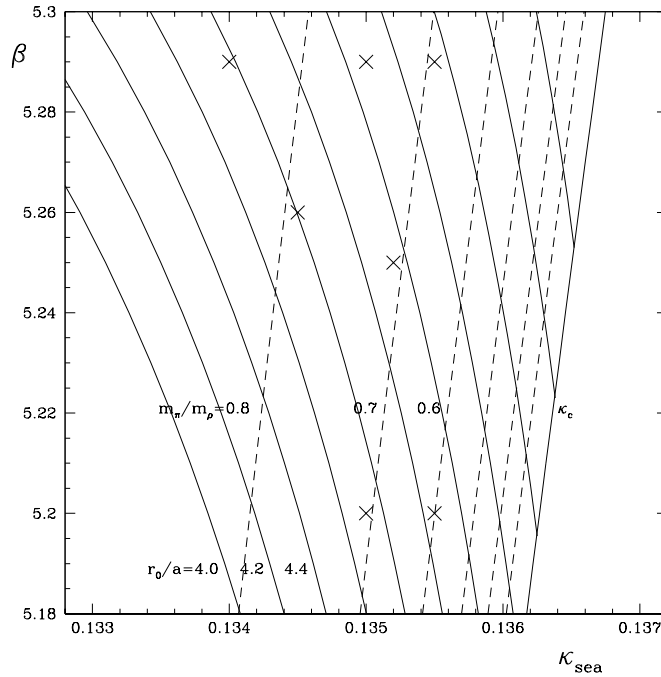


Fig. 3. Lines of constant  $r_0=a$  (full lines), from 4.0 (left) to 6.0 (right), and constant  $m = m_p$  (dashed lines), from 0.8 to 0.3, together with  $\kappa_c$  and the parameters ( ) of our simulations (up to now) in the  $(\kappa_{sea}, \beta)$  plane. The curves are from a fit to the renormalization group and chiral perturbation theory, respectively.

where we have neglected terms of  $O((m r_0)^2)$ , which we will justify later on. Note that effectively  $\frac{N_f}{M S} r_0$  can be written as a function of  $m r_0$  and  $a=r_0$ .

Let us now turn to the fit and extrapolation of our data. In the fit we assume that  $\frac{N_f}{M S} r_0$ ,  $a$  and  $r_0=a$  are uncorrelated. We find that the ansatz (29) fits the data very well ( $\chi^2 = 3.1$ ). The parameters  $B$  and  $C$  are strongly correlated though, indicating that it does not matter whether we are using  $a$  or  $m r_0$  as the chiral extrapolation variable. Indeed, fixing  $C = 0$  gives the same result for  $A$  and an almost identical value of  $\chi^2$ . If our ansatz (29) is correct, then a plot of  $\frac{N_f}{M S} r_0 (m = 0) = \frac{N_f}{M S} r_0 (A (B a m + C m r_0 + B C a m m r_0))$  against  $(a=r_0)^2$  should collapse all the data points onto a single line,  $A + D (a=r_0)^2$ , if the correct  $A$ ,  $B$  and  $C$  values are used. Similarly, a plot of  $\frac{N_f}{M S} r_0 (a = 0) = (\frac{N_f}{M S} r_0 - D (a=r_0)^2) = (1 + B a m)$  against  $m r_0$  should collapse the data onto the line  $A (1 + C m r_0)$  if the correct  $B$  and  $D$  values are chosen. This is what we have plotted in Figs. 4 and 5. We see that it does indeed bring all data points onto one line. We also see that the deviations from the line are probably not statistically significant, so adding any extra term to the fit, like  $(m r_0)^2$ , the deviation from the line is just going to give a fit to the noise. Note that the slope of the line in Fig. 4 is very similar to the slope of the corresponding quenched line in Fig. 2.

In the chiral and continuum limit our fit gives

$$\frac{N_f=2}{M S} r_0 = 0.549(39) \quad (28)$$

The first error is purely statistical, while the second one is an estimate of the systematic error, where we again have assumed that the higher-order contributions in eq. (26) are about 20% of the  $O(g^6)$  term. Using  $r_0 = 0.5$  fm, this gives

$$\frac{N_f=2}{M S} = 217(16)(11) \text{ MeV} \quad (31)$$

A preliminary analysis of our dynamical data indicates that using either the nucleon mass, or even the pion mass, to set the scale gives results that are consistent with the  $r_0$  value used.

### Comparison with Phenomenology

How can our results be compared with the phenomenological numbers? A fit to the world data of  $\alpha_s$  gives the average value at the Z mass [1]  $\frac{N_f=5}{M S} (m_Z) = 0.118(2)$ , which corresponds to  $\frac{N_f=5}{M S} = 208(25) \text{ MeV}$ . The latter value refers to an idealized world of five massless quarks and thus cannot be compared immediately to our numbers. We may extrapolate  $\frac{N_f}{M S} r_0$  to three flavors (remember that  $r_0$  is extracted from the phenomenological heavy quark potential) and then evolve the corresponding  $\frac{N_f}{M S}$  to the Z mass, using the three-loop matching formulae [35]. We do this by extrapolating  $\ln(\frac{N_f}{M S} r_0)$  linearly in  $N_f$  to  $N_f = 3$ , ignoring the fact that the strange quark mass is

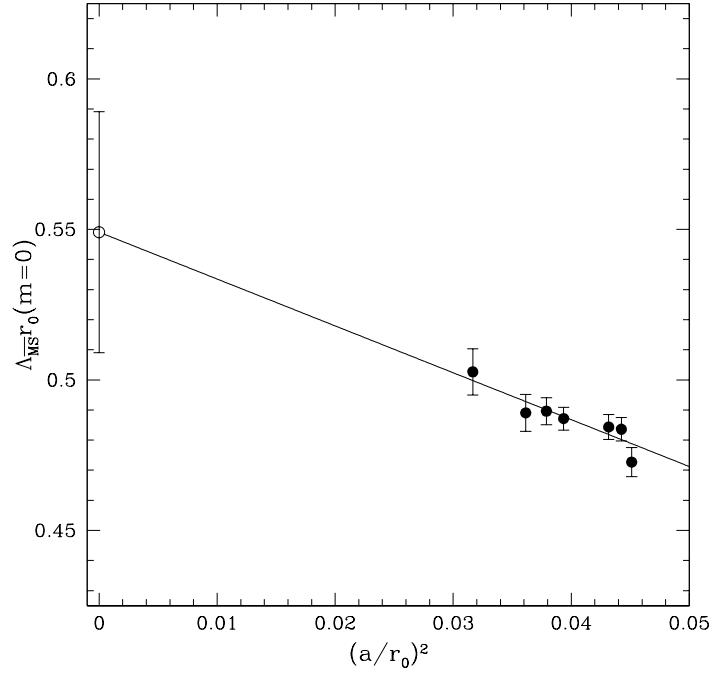


Fig. 4. The scale parameter  $\frac{\Delta}{M S} r_0$  ( $m = 0$ ) against  $(a=r_0)^2$  together with the t (29) and the continuum result (30). The error of (30) shown is the statistical error only.

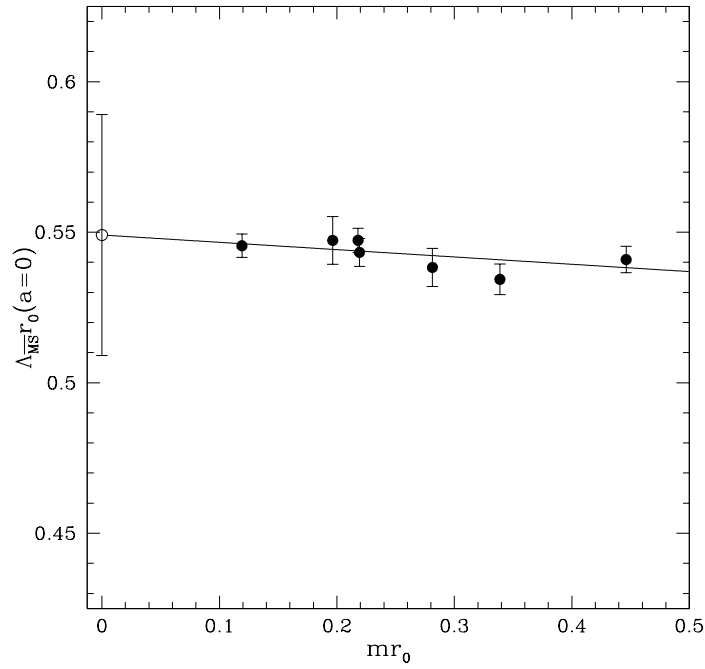


Fig. 5. The scale parameter  $\frac{\Delta}{M S} r_0$  ( $a = 0$ ) against  $am$  together with the t (29) and the continuum result (30).

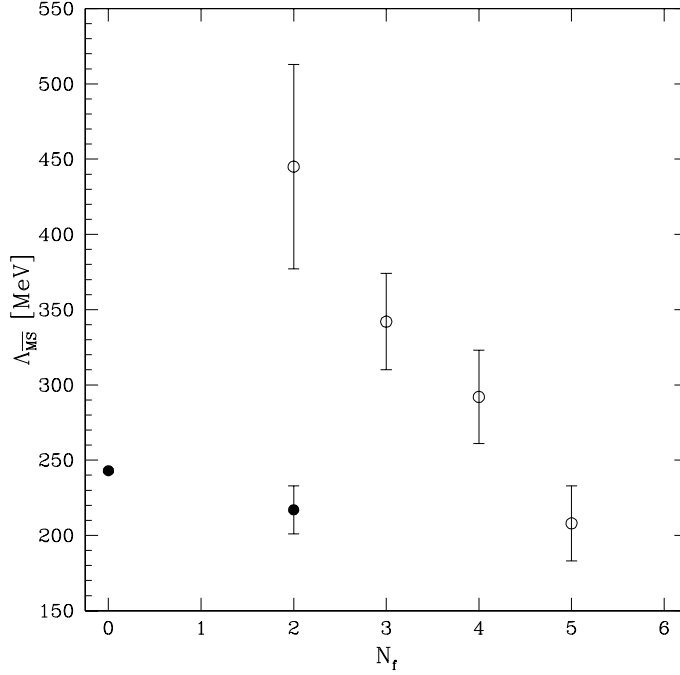


Fig. 6. The lattice ( ) and phenomenological ( ) scale parameters  $\Lambda_{\overline{MS}}$  against  $N_f$ . The error bars of the lattice numbers correspond to the statistical errors.

already relatively heavy and therefore less effective. For  $r_0 = 0.5$  fm this gives  $\frac{N_f=3}{M S} = 205(22)(20)$  MeV. With the help of eq. (7) we now compute  $\frac{N_f=3}{M S}$  at the scale  $\mu = 1$  GeV and obtain  $\frac{N_f=3}{M S}(1 \text{ GeV}) = 0.330(21)(19)$ . Taking the charm and bottom thresholds to be at 1.5 GeV and 4.5 GeV, respectively, we then find  $\frac{N_f=5}{M S}(m_Z) = 0.1076(20)(18)$ , a number which is somewhat lower than the phenomenological value. If, on the other hand, we evolve the phenomenological value down to  $N_f = 4$  and  $N_f = 3$ , we obtain  $\frac{N_f=4}{M S} = 292(31)$  MeV and  $\frac{N_f=3}{M S} = 342(32)$  MeV, respectively. A logarithmic extrapolation to  $N_f = 2$ , similar to our extrapolation of the lattice data but in reverse order, would give  $\frac{N_f=2}{M S} = 445(68)$  MeV.

In Fig. 6 we compare the values obtained by the various methods. At energy scales below the charm mass threshold the physics should be determined by  $\frac{N_f=3}{M S}$ . So one would expect that the lattice numbers extrapolate smoothly to the corresponding phenomenological value. We see, however, that this is not the case. The reason for this mismatch remains to be found.

#### 4 Conclusions

Our quenched result agrees very well with results of other calculations using different methods. We find significant  $O(a^2)$  corrections. For example at  $\beta = 6.0$ , corresponding to a lattice spacing  $a = 0.1$  fm, they amount to 10%, which makes an extrapolation of the results to the continuum limit

indispensable. In the dynamical case the data cover a much smaller range of  $a$ , which makes the extrapolation to the continuum limit less reliable. But it is reassuring to see that the continuum limit is approached at a similar rate as in the quenched case.

Our dynamical calculation is similar in spirit to previous unquenched computations of  $\beta$  [11-14] (albeit not exactly the same). The main differences are that we are using a non-perturbatively  $O(4)$  improved fermion action, which reduces cut-off effects, the conversion to  $\overline{MS}$  is done consistently in two-loop perturbation theory, and an extrapolation of  $\beta$  to the chiral and continuum limit is performed.

## Appendix

We follow the argument in [34] calculating the relation between the parameters from the potential. We require that the potential (or force) between two static charges should be the same, whether computed as a series in  $g^2$  or  $g_{\overline{MS}}^2$ . All we have to do to calculate the fermionic piece of the relation is to compute the fermionic contribution to the gluon propagator.

In the scheme  $S$  we have

$$V(\mathbf{x}) = \int \frac{d^4q}{(2\pi)^4} 2 \frac{(q) g_S^2}{q^2} \left[ 1 + \frac{3}{2} G^S(q^2) + \frac{3}{2} N_f \Pi^S(q^2; m) + O(g_S^4) e^{i\mathbf{q}\mathbf{x}} \right]; \quad (32)$$

where  $G^S(q^2)$  is the one-loop gluon contribution to the potential, and  $\Pi^S$  is the one-loop quark vacuum polarization. If two schemes,  $S$  and  $S^0$ , are to give the same answer for  $V(\mathbf{x})$ , their couplings have to be related by

$$\frac{1}{g_S^2} = \frac{1}{g_{S^0}^2} + \frac{3}{2} \frac{G^{S^0}(q^2) - G^S(q^2) + N_f \Pi^{S^0}(q^2; m) - \Pi^S(q^2; m) + O(g^2)}{g_{S^0}^2}; \quad (33)$$

To find the fermionic part of the conversion from  $g^2$  to  $g_{\overline{MS}}^2$ , we have to calculate the vacuum polarization in both schemes and take the difference.

In the  $\overline{MS}$  scheme we find

$$\overline{MS} \Pi(q^2; m) = \frac{1}{24} \frac{1}{m^2} \ln(q^2 = m^2) - \frac{5}{3} + O(m^2 = q^2); \quad (34)$$

On the lattice we obtain

$$\begin{aligned}
(\alpha^2; m) = & \frac{1}{24} \ln(a^2 q^2) - 3am (1 - c_{SW}) \ln(a^2 q^2) \\
& 3.25275141(5) + 1.19541770(1)c_{SW} - 7.06903716(4)c_{SW}^2 \\
& + am (6.46270704(30) - 5.29413266(6)c_{SW} \\
& + 1.67389761(2)c_{SW}^2) :
\end{aligned} \tag{35}$$

We see that there is an unwanted  $am \ln(a^2 q^2)$  term in eq. (35) unless  $c_{SW} = 1 + O(g^2)$ . Combining our calculation of  $t_1$  with the calculation of the purely gluonic part in the literature [22], we get our final result for  $t_1$  (for general  $N_c$ ):

$$\begin{aligned}
t_1 = & 0.16995600 N_c \frac{1}{8N_c} \\
& N_f (0.00669600 - 0.00504671 c_{SW} + 0.02984347 c_{SW}^2) \\
& + am (0.02728371 + 0.02235032 c_{SW} - 0.00706672 c_{SW}^2) :
\end{aligned} \tag{36}$$

The  $am$  term in eq. (36) means that in dynamical QCD the contours of constant  $\frac{q^2}{M_S^2}(l=a)$  will be slanted when plotted in a  $(am; )$  plane. As one expects the contours of constant  $r_0=a$  to roughly follow contours of constant  $\frac{q^2}{M_S^2}(l=a)$ , this term gives a possible explanation of the appearance of the sloped lines in Fig. 3.

Acknowledgement

We thank H. Panagopoulos for communicating the three-loop  $\beta$  function for improved Wilson fermions to us prior to publication. The numerical calculations have been performed on the Hitachi SR8000 at LRZ (Munich), on the Cray T3E at EPCC (Edinburgh), NIC (Julich) and ZIB (Berlin) as well as on the APE/Quadrics at DESY (Zeuthen). We thank all institutions for their support. This work has been supported in part by the European Community's Human Potential Program under contract HPRN-CT-2000-00145, Hadrons/Lattice QCD. MG and PELR acknowledge financial support from DFG.

## References

- [1] Particle Data Group, Eur. Phys. J. C 15 (2000) 1.
- [2] P. Weisz, Nucl. Phys. B (Proc. Suppl.) 47 (1996) 71.
- [3] J. Shigemitsu, Nucl. Phys. B (Proc. Suppl.) 53 (1997) 16.

- [4] S.P. Booth, D.S. Henty, A. Hulsebos, A.C. Irving, C. Michael and P.W. Stephenson, *Phys. Lett. B* 294 (1992) 385.
- [5] G.S. Bali and K. Schilling, *Phys. Rev. D* 47 (1993) 661.
- [6] R.G. Edwards, U.M. Heller and T.R. Klassen, *Nucl. Phys. B* 517 (1998) 377.
- [7] J.I. Skullerud, *Nucl. Phys. B (Proc. Suppl.)* 63 (1998) 242.
- [8] B. Alles, D.S. Henty, H. Panagopoulos, C. Parrinello, C. Pittori and D.G. Richards, *Nucl. Phys. B* 502 (1997) 325.
- [9] P. Boucaud, G. Burgio, F. DiRenzo, J.P. Leroy, J. Micheli, C. Parrinello, O. Pene, C. Pittori, J. Rodriguez-Quintero, C. Roiesnel and K. Sharkey, *JHEP* 0004 (2000) 006.
- [10] A.X. ElKhadra, G. Hockney, A.S. Kronfeld and P.B. Mackenzie, *Phys. Rev. Lett.* 69 (1992) 729.
- [11] S. Aoki, M. Fukugita, S. Hashimoto, N. Ishizuka, H. Mino, M. Okawa, T. Onogi and A. Ukawa, *Phys. Rev. Lett.* 74 (1995) 22.
- [12] M. Wingate, T. DeGrand, S. Collins and U.M. Heller, *Phys. Rev. D* 52 (1995) 307.
- [13] C.T.H. Davies, K. Hombostel, G.P. Lepage, P. McCallum, J. Shigemitsu and J. Sloan, *Phys. Rev. D* 56 (1997) 2755.
- [14] A. Spitz, H. Hoerber, N. Eicker, S. Gusken, T. Lippert, K. Schilling, T. Struckmann, P. Ueberholz and J. Vieho, *Phys. Rev. D* 60 (1999) 074502.
- [15] S. Capitani, M. Luscher, R. Sommer and H. Wittig, *Nucl. Phys. B* 544 (1999) 669.
- [16] R. Sommer, *Nucl. Phys. B* 411 (1994) 839.
- [17] B. Sheikholeslami and R. Wohlert, *Nucl. Phys. B* 259 (1985) 572.
- [18] K. Jansen and R. Sommer, *Nucl. Phys. B* 530 (1998) 185.
- [19] T. van Ritbergen, J.A.M. Vermaseren and S.A. Larin, *Phys. Lett. B* 400 (1997) 379; J.A.M. Vermaseren, S.A. Larin and T. van Ritbergen, *Phys. Lett. B* 405 (1997) 327.
- [20] G. Parisi, in *High Energy Physics – 1980, Proceedings of the XXth International Conference*, Madison, eds. L. Durand and L.G. Pondrom (American Institute of Physics, New York, 1981); G.P. Lepage and P.B. Mackenzie, *Phys. Rev. D* 48 (1993) 2250.
- [21] F. DiRenzo, G. Marchesini and E. Onofri, *Nucl. Phys. B* 457 (1995) 202; F. DiRenzo and L. Scorzato, hep-lat/0011067.
- [22] M. Luscher and P. Weisz, *Phys. Lett. B* 349 (1995) 165; M. Luscher, hep-lat/9802029.

- [23] B. Alles, A. Feo and H. Panagopoulos, *Phys. Lett. B* 426 (1998) 361.
- [24] S. Sint, private notes (1996), quoted in A. Bode, P. Weisz and U. Wol, *Nucl. Phys. B* 576 (2000) 517.
- [25] L. Marcantonio, P. Boyle, C. T. H. Davies, J. Hein and J. Shigemitsu, *Nucl. Phys. B (Proc. Suppl.)* 94 (2001) 363.
- [26] A. Bode and H. Panagopoulos, to be published.
- [27] M. Gockeler, R. Horsley, H. Perlt, P. E. L. Rakow, G. Schierholz, A. Schiller and P. Stephenson, *Phys. Rev. D* 57 (1998) 5562; M. Gockeler, R. Horsley, D. P. Leiter, P. E. L. Rakow, G. Schierholz and P. Stephenson, *Nucl. Phys. B (Proc. Suppl.)* 83 (2000) 203.
- [28] D. P. Leiter, Thesis, Berlin (2000); QCD SF C Collaboration, in preparation.
- [29] M. Guagnelli, R. Sommer and H. Wittig, *Nucl. Phys. B* 535 (1998) 389.
- [30] H. Stuben, *Nucl. Phys. B (Proc. Suppl.)* 94 (2001) 273.
- [31] A. C. Irving, *Nucl. Phys. B (Proc. Suppl.)* 94 (2001) 242.
- [32] C. R. Allton et al., UKQCD Collaboration, in preparation.
- [33] D. P. Leiter, *Nucl. Phys. B (Proc. Suppl.)* 94 (2001) 265.
- [34] I. Montvay and G. Münster, *Quantum Fields on a Lattice* (Cambridge Univ. Press, Cambridge, 1994).
- [35] K. G. Chetyrkin, J. H. Kühn and M. Steinhauser, *Comput. Phys. Commun.* 133 (2000) 43.